MEASUREMENT OF ANGULAR MOTIONS USING PIEZOCERAMIC BIMORPHS

Cicogna, T. R., thcic@sc.usp.br
Varoto, P. S., varoto@sc.usp.br
Trindade, M. A., trindade@sc.usp.br
Engineering School of São Carlos, Departament of Mechanical Engineering, University of São Paulo.
Av. Trabalhador São Carlense, nº. 400, Sao Carlos, S.P, Brazil. CEP: 13566-590.

Abstract. *Accurate measurement of angular motions is important for a class of modal testing applications. Although these quantities can be determined either through expansion of the translational motions or through a direct measurement by employing angular accelerometers, there is still need for low cost and reliable alternative techniques to quantitatively assess the angular motions in the structure under test. A recently proposed technique using low cost PZT transducers seems quite interesting since it uses bimorph piezoceramic patches to measure the structure´s local curvature through measurement of the electric potential induced by the extension and compression of the patch´s top and bottom stripes, respectively. From this curvature, rotation can be obtained directly by interpolation. In this work, a finite element model for the dynamic analysis is proposed to evaluate some important characteristics of bimorphs patches applied to the measurement of angular degrees of freedom, which are: i) for one-dimensional structures, like a beam, the length of the PZT; and ii) the position of the sensor. Numerical results are compared with experimental data considering a cantilever beam as the tested structure. The present study may help to establish a simple and efficient piezoelectric rotational sensor leading to a significant improvement on the estimation of the structure´s complete FRF response matrix.*

Keywords*: angular motions, piezoelectric materials, experimental modal analysis, angular FRF*

1. INTRODUCTION

Rotational degrees of freedom (RDOFs) have to be taken into account in many areas of structural dynamic analyses as independent co-ordinates. However, the possibilities for measuring RDOFs are so limited that in some cases, the attempt has to given up and confined to the measured translational degrees of freedom (TDOFs) only (Liu and Ewins, 1999).

Several methods have been investigated in order to measure the rotational response. Based on the following ideas: i) angular measurements using dedicated sensors based on gyroscopic sensors (Algrain, 1991) and using magnetohydrodynamic sensors (Laughling *et al.*, 1992); ii) curve fitting where the data measured directly on the vibrating structure in the proximity of the point of interest are fitted with curves (polynomial, splines) in the mono-dimensional case or (bi-cubic surfaces) in the bi-dimensional case (Ng'andu *et al.*, 1993); iii) the use of laser vibrometers in angular measurement of vibrations (Bokelberg *et al.*, 1993); iv) pseudo-rotational transducer comprised of an array of two or more translational accelerometers (Yoshimura and Hosoya, 2000) and differentiation of translational data (Duarte and Ewins, 2000) and v) PZT transducers (bimorph) that are able to estimate rotational quantities (Bello *et al.*, 2003).

For a general structure the input at an arbitrary point q consists of two vectors: a force and a moment vector. The first three components F_1, F_2 and F_3 are forces in the x, y, z directions, respectively. The remaining components F_4, F_5 and F_6 are moments about the x, y, z directions, respectively. The structure's output response at the pth point consists of two vectors: a vector of linear motions (displacements, velocities or accelerations) and a vector of angular motions (displacements, velocities or accelerations). Consequently, the output motion vector at location p has six components like the input at location q has six components as well. Thus, between each pair of input-output points p and q on the structure, there are potentially 36 input/output FRF relationships (Varoto, 1996).

Although rotational degrees of freedom can be included in finite element models, experimental FRFs do not because of the difficulty of their measurement. Besides, is not possible yet to apply and measure lumped moments to the structure to determine the sub-matrices $[H_{FM}]$ and $[H_{MM}]$, some strategies could be developed to estimate or measure $[H_{MF}]$ and consequently $[H_{FM}]$, because of the symmetry condition.

In this paper, the use of low cost PZT patches (bimorph), which are able to measure the local curvature of a structure, is considered. From it, rotational quantities (rotation) can be obtained either by integration or by interpolation techniques. In such case, 75% of the total structure FRF matrix could be determined. Analytical modes method was considered to the approximation. A methodology based on genetic algorithm is also presented to find the optimal bimorph's size and position. The bimorph's results are compared with an angular accelerometer for a cantilever beam.

2. THEORETICAL FORMULATION

A laminate beam with elastic and/or piezoelectric layers is considered. The beam is modelled using classical laminate theory that is all layers are subjected to the same displacements field and Euler–Bernoulli assumptions are considered. The piezoelectric layers are supposed transversely poled and subject to transverse electrical fields and elastic layers are assumed insulated. All layers are assumed perfectly bonded and in plane stress state. The length, width and thickness of the beam are denoted by L, b and h, respectively.

Axial displacements $\overline{u}(x,z,t)$ are assumed linear, whereas transverse ones $\overline{w}(x,z,t)$ are supposed constant through thickness.

$$\overline{u}(x,z,t) = u(x,t) - z\beta(x,t),\ \overline{w}(x,z,t) = w(x,t) \tag{1}$$

Notice that the same displacements fields $\overline{u}$ are considered for all layers. From Euler-Bernoulli hypotheses, $\beta(x,t) = -w'$, where $\bullet'$ is used to denote $\partial\bullet/\partial x$. The bottom-plan of the bottom layer (beam) is set to coincide with the origin of the z-axis.

Using the usual strain-displacement relations for each layer, the axial ε_1 strain can be written as:

$$\varepsilon_1 = \varepsilon^m + z\varepsilon^b \tag{2}$$

where $\varepsilon^m = u'$ and $\varepsilon^b = -w''$.

The superscripts m, b state for membrane and bending strains. A constant transverse electrical field is assumed for the piezoelectric layers and the remaining in-plane components are supposed to vanish. Although electrostatic equilibrium equation is only satisfied with a linear electrical field assumption (Rahmoune *et al*., 1998), it seems that the linear part should be negligible for the kind of problems treated in this work (Trindade *et al.*, 2001). Consequently it is, for the j th piezoelectric layer,

$$E_3^j = -\frac{V_j}{h_j} \tag{3}$$

where V_j is the difference of electric potential of the j th laminae, defined by $V_j = V_j^+ - V_j^-$, where V_j^+ and V_j^- are the voltages applied on the upper and lower skins of the j th piezoelectric layer.

2.1. Reduced constitutive equations

Linear orthotropic piezoelectric materials with material symmetry axes parallel to those of the beam are considered. c_{ij}, e_{lj} and $\in_{ll}$ ($i,j = 1,\ldots,6$; $l = 1,2,3$) denote their elastic, piezoelectric and dielectric constants. For simplicity of notation, all layers will be considered piezoelectric. Elastic layers are obtained by making their piezoelectric constants vanish. Due to the plane stress assumption, the three-dimensional linear constitutive equations of an orthotropic piezoelectric layer can be reduced to (Benjeddou *et al.*, 1997)

$$\begin{bmatrix} \sigma_1^j \\ D_3^j \end{bmatrix} = \begin{bmatrix} \overline{c}_{11}^j & -\overline{e}_{31}^j \\ \overline{e}_{31}^j & \overline{\in}_{33}^j \end{bmatrix} \begin{bmatrix} \varepsilon_1 \\ E_3^j \end{bmatrix} \tag{4}$$

where

$$\overline{c}_{11} = c_{11} - \frac{c_{13}^2}{c_{33}},\ \overline{e}_{31} = e_{31} - \frac{c_{13}}{c_{33}}e_{33},\ \overline{\in}_{33} = \in_{33} + \frac{e_{33}^2}{c_{33}}$$

σ_1 and D_3 are axial stress and transverse electrical displacement. Notice that electromechanical coupling in the piezoelectric face sublayers is between axial strain and transverse electrical field. This is the conventional piezoelectric extension actuation mechanism.

2.2. Variational formulation

Using d'Alembert's principle, the following variational equation can be written for the piezoelectric laminated beam

$$\delta T - \delta H + \delta W = 0\,,\ \forall \delta u, \delta w, \delta V_j \tag{5}$$

where δT, δH and δW are the virtual work of inertial, electromechanical internal and applied mechanical forces, respectively.

The electromechanical internal forces virtual work of the piezoelectric laminate beam is

$$\delta H = \sum_j \delta H_j \tag{6}$$

where

$$\delta H_j = \int_{\Omega_j} \left(\sigma_1^j \delta \varepsilon_1 - D_3^j \delta E_3^j \right) d\Omega_j$$

with Ω_j being the volume of the j th layer.

Using constitutive equations (4), strain (2) and electrical field (3) relations, then integrating through the cross-sectional area, the above equations, for the j th piezoelectric layer, become

$$\begin{aligned} \delta H_j = \int_0^L \Bigg[& \delta u' \left(\bar{c}_{11}^j A_j u' - \bar{c}_{11}^j \bar{I}_j w'' + \bar{e}_{31}^j \frac{A_j V_j}{h_j} \right) + \delta w'' \left(-\bar{c}_{11}^j \bar{I}_j u' + \bar{c}_{11}^j I_j w'' - \bar{e}_{31}^j \bar{I}_j \frac{V_j}{h_j} \right) \\ & + \frac{\delta V_j}{h_j} \left(\bar{e}_{31}^j A_j u' - \bar{e}_{31}^j \bar{I}_j w'' - \bar{\in}_{33}^j A_j \frac{V_j}{h_j} \right) \Bigg] dx \end{aligned} \tag{7}$$

Notice that there are membrane-bending coupling terms due to the multilayer characteristic of the beam. A_j, $\bar{I}_j$ and I_j are, respectively, the area and the first and second moments of area of the j th layer cross-section. These are

$$\left[A_j, \bar{I}_j, I_j \right] = \int_{z_j}^{z_j + h_j} \int_{z_j}^{z_j + h_j} \left[1, z, z^2 \right] dz dy \tag{8}$$

where the local z -axis of the j th layer is situated at its bottom plan, such that

$$z_j = \sum_{i=1}^{j-1} h_i$$

The inertial forces virtual work of the laminate beam is

$$\delta T = \sum_j \delta T_j \tag{9}$$

where

$$\delta T_j = -\int_{\Omega_j} \left[\rho_j \left(\delta \bar{u}\, \ddot{\bar{u}} + \delta \bar{w}\, \ddot{\bar{w}} \right) \right] d\Omega_j$$

with ρ_j being the volume mass density of the j th layer and $\dot{\bullet}$ stating for $\partial \bullet / \partial t$. Using the displacements relations (1) and integrating through the cross-sectional area, the above equation become

$$\delta T_j = -\int_0^L \rho_j A_j \left(\delta u \ddot{u} + \delta w \ddot{w} \right) dx \tag{10}$$

Notice that the rotary inertia and the translation-rotation inertial coupling terms are neglected to simplify the model.

The virtual work of axial and transversal forces applied to each layer can be written as

$$\delta W = \sum_j \delta W_j \tag{11}$$

where

$$\delta W_j = \int_0^L \left(\delta u N_j + \delta w V_j + \delta w' M_j\right) dx \tag{12}$$

where N_j, V_j and M_j are the normal, transversal and moment resultants applied to the j th layer.

2.3. Equations of motion

The equations of motion for the entire beam could be written by

$$\sum_j \left(\delta T_j - \delta H_j + \delta W_j\right) = 0\ ,\ \forall \delta u,\ \delta w, \delta V_j \tag{13}$$

Using the relations in (7), (9) and (11) the above equation becomes

$$\begin{aligned}\int_0^L \Bigg\{ \delta u \Bigg[\left(-\sum_j \rho_j A_j \right) \ddot{u} + \left(\sum_j \bar{c}_{11}^j A_j \right) u'' - \left(\sum_j \bar{c}_{11}^j \bar{I}_j \right) w''' + N_j \Bigg] + \delta w \Bigg[\left(-\sum_j \rho_j A_j \right) \ddot{w} + \left(\sum_j \bar{c}_{11}^j \bar{I}_j \right) u''' \\ - \left(\sum_j \bar{c}_{11}^j I_j \right) w''' \Bigg] + \sum_j \frac{\delta V_j}{h_j} \left(\bar{e}_{31}^j A_j u' - \bar{e}_{31}^j \bar{I}_j w'' - \bar{\in}_{33}^j A_j \frac{V_j}{h_j} \right) \Bigg\} dx = 0\end{aligned} \tag{14}$$

Notice that, in despite of the Euler-Bernoulli hypotheses where u and w are the same for each layer, the differences of electric potential V_j of each layer are independent. Hence, the equations of motion become

$$\left(\sum_j \rho_j A_j \right) \ddot{u} - \left(\sum_j \bar{c}_{11}^j A_j \right) u'' + \left(\sum_j \bar{c}_{11}^j \bar{I}_j \right) w''' = N_j \tag{15a}$$

$$\left(\sum_j \rho_j A_j \right) \ddot{w} + \left(\sum_j \bar{c}_{11}^j I_j \right) w'''' - \left(\sum_j \bar{c}_{11}^j \bar{I}_j \right) u''' = V_j - M_j' \tag{15b}$$

$$\bar{e}_{31}^j A_j u' - \bar{e}_{31}^j \bar{I}_j w'' - \bar{\in}_{33}^j A_j \frac{V_j}{h_j} = 0 \tag{15c}$$

Since we are interested in evaluating the unknown electric potential induced at a piezoelectric sensor by the vibration of the structure, Eq. (15c) could be solved for V_j leading to

$$V_j = \frac{\bar{e}_{31}^j}{\bar{\in}_{33}^j} \left(h_j u' - \frac{h_j \bar{I}_j}{A_j} w'' \right) \tag{16}$$

Notice that equation (16) is the reason to use bimorph sensors. With only one piezoelectric patch it is not possible to determine the voltage only from the curvature w'' since it is also dependent of the axial displacement. However, if we make use of an identical pair of piezoelectric patches bonded on each other (bimorph), we may write that

$$V_2 - V_1 = \frac{\bar{e}_{31}}{\bar{\in}_{33}} \frac{h}{A} \left(\bar{I}_1 - \bar{I}_2 \right) \tag{17}$$

where for piezoelectric patches with rectangular cross-section

$$V_2 - V_1 = -\frac{\bar{e}_{31}}{\bar{\epsilon}_{33}} h^2 w'' \tag{18}$$

Finally, the local curvature could be directly associated with the voltage measured from each bimorph by

$$w''(x,t) = -\frac{\bar{\epsilon}_{33}}{\bar{e}_{31}} \frac{[V_2(t) - V_1(t)]}{h^2} \tag{19}$$

3. GETTING ROTATIONS FROM PZT BIMORPH MEASUREMENTS

To determine rotation from the local curvature measured using the bimorph transducer one approximation method is proposed in what follows.

3.1. Analytical modes interpolation

Using analytical modes for interpolation, the beam displacement field can be approximated by:

$$\begin{aligned}
w(x,t) &= \sum_{i=1}^{N} \phi_i(x)\alpha_i(t) = \alpha_i(t)\left[a_p^{(i)}x^p + a_{p-1}^{(i)}x^{p-1} + \cdots + a_3^{(i)}x^3 + a_2^{(i)}x^2 + a_1^{(i)}x + a_0^{(i)}\right] \\
w'(x,t) &= \sum_{i=1}^{N} \alpha_i(t)\phi_i'(x) = \alpha_i(t)\left[pa_p^{(i)}x^{p-1} + (p-1)a_{p-1}^{(i)}x^{p-2} + \cdots + 3a_3^{(i)}x^2 + 2a_2^{(i)}x + a_1^{(i)}\right] \\
w''(x,t) &= \sum_{i=1}^{N} \alpha_i(t)\phi_i''(x) = \alpha_i(t)\left[p(p-1)a_p^{(i)}x^{p-2} + (p-1)(p-2)a_{p-1}^{(i)}x^{p-3} + \cdots + 6a_3^{(i)}x + 2a_2^{(i)}\right]
\end{aligned} \tag{20}$$

where $\phi_i(x)$ represents the i th analytic modal shape for a cantilever Euler-Bernoulli beam. In such case, the terms $a_j^{(i)}$ ($j = 0, \ldots p$) can be evaluated for a given polynomial order p.

The analytical modes coefficients $\alpha_i(t)$ can be determined by enforcing the structure's four boundary conditions and the curvatures, evaluated from the voltages induced on the bimorph sensors, at N measurement locations for each time instant t_i. However, having assumed N bimorph sensors, the total number of coefficients that can be determined is $N+2$, since the geometric boundary conditions are already embedded into the analytical modes shapes.

According to (20) and boundaries conditions for a cantilever beam, the system could be written by

$$\begin{bmatrix} \phi_1''(x_b) & \phi_2''(x_b) & \cdots & \phi_{N+2}''(x_b) \\ \vdots & \vdots & \vdots & \vdots \\ \phi_1''(L) & \phi_2''(L) & \cdots & \phi_{N+2}''(L) \\ \phi_1'''(L) & \phi_2'''(L) & \cdots & \phi_{N+2}'''(L) \end{bmatrix} \begin{Bmatrix} \alpha_1(t_i) \\ \vdots \\ \alpha_{N+1}(t_i) \\ \alpha_{N+2}(t_i) \end{Bmatrix} = \begin{Bmatrix} w_b''(x_b, t_i) \\ \vdots \\ 0 \\ 0 \end{Bmatrix} \tag{21}$$

Notice that the total number of modes that can be used into the approximation is equal to $N+2$, since we have to write a square matrix to solve the system of equations (21).

Finally, the rotation at a position x_{out} can be approximated by

$$w'(x_{out}, t) = \alpha_1(t)\phi_1'(x_{out}) + \alpha_2(t)\phi_2'(x_{out}) + \ldots + \alpha_{N+1}(t)\phi_{N+1}'(x_{out}) + \alpha_{N+2}(t)\phi_{N+2}'(x_{out}) \tag{22}$$

4. NUMERICAL RESULTS

A Matlab® program was developed according to assumptions made previously to determine rotational FRFs for an aluminum cantilever beam with dimensions $500 \times 25 \times 3\ \text{mm}^3$. The beam was excited by a transversal force at its free end in the 0-500 Hz frequency range (Figure 1).

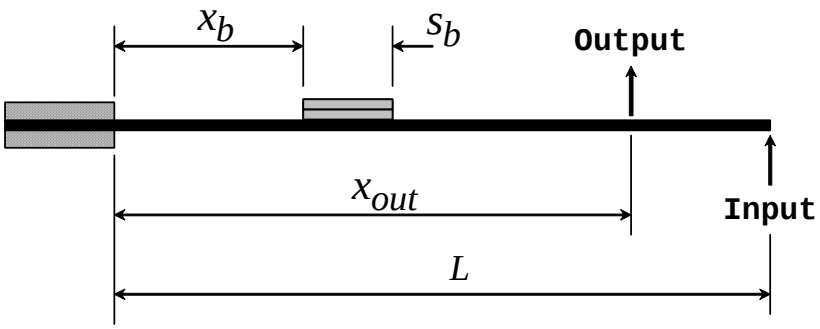

Figure 1. Configuration of the numerical set-up

In order to provide a quantitative comparison, an overall error term (fitness) was created to be used for comparisons between angular FRFs (FRFA) from finite element and bimorph results (Cafeo *et al*., 1992).

$$fitness = 10\left(\sqrt{\frac{\sum\left(20\log_{10}\left(FRFA_{bimorph}\right)-20\log_{10}\left(FRFA_{finite\_element}\right)\right)^2}{N}}\right)^{-1} \tag{23}$$

where N represents the number of points into the range of analysis.

Figure 2 shows the necessity of optimize the bimorph's pair: length-position. It could be observed that for a specific output response point (x_{out}) there is a great change for the fitness function in terms of the position of the bimorph sensor along the beam and in terms of bimorph's length.

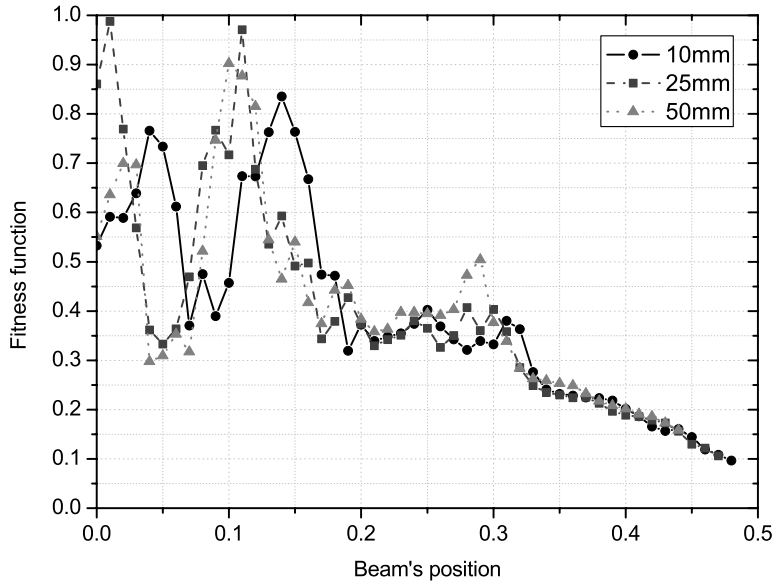

Figure 2. Fitness function according to 3 types of bimorph's length and beam's position

4.1. Optimization using genetic algorithms

Genetic Algorithms (GAs) are adaptive heuristic search algorithm premised on the evolutionary ideas of natural selection and genetic. The basic concept of GAs is designed to simulate processes in natural system necessary for evolution, specifically those that follow the principles first laid down by Charles Darwin of survival of the fittest.

In this paper, genetic algorithm was used for optimal placement and sizing of the bimorph on a cantilever beam considering the fitness function presented in (23). A simple genetic algorithm based on binary basis was used with the

following configuration: population size = 30; mutation rate = 0.05, crossover rate = 1.00 with one-point brake and chromosome with 14 bits: 6 bits for bimorph's position and 8 bits for bimorph's length.

Figures 3 and 4 presents best, average and worst fitness evolution and optimal results for two different beam's point response: $x_{out} = 100$ mm and $x_{out} = 250$ mm. The optimal locations and size were found as follows: $x_{b1} = 27$ mm, $s_{b1} = 29$ mm and $x_{b2} = 177$ mm, $s_{b2} = 25$ mm, respectively.

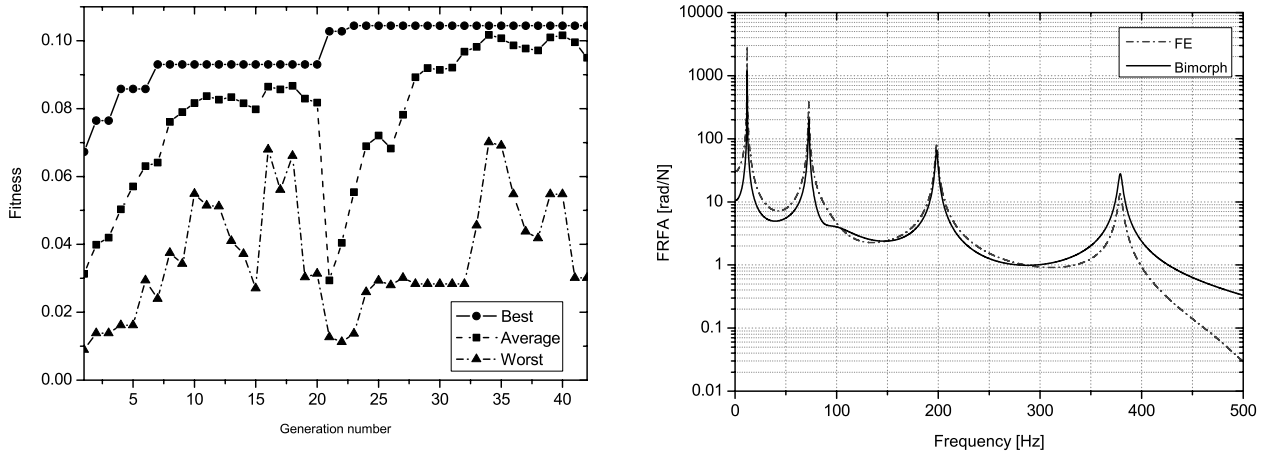

Figure 3. Fitness evolution and comparison between FE (---) and bimorph (—) angular FRFs for beam angular response at 100mm

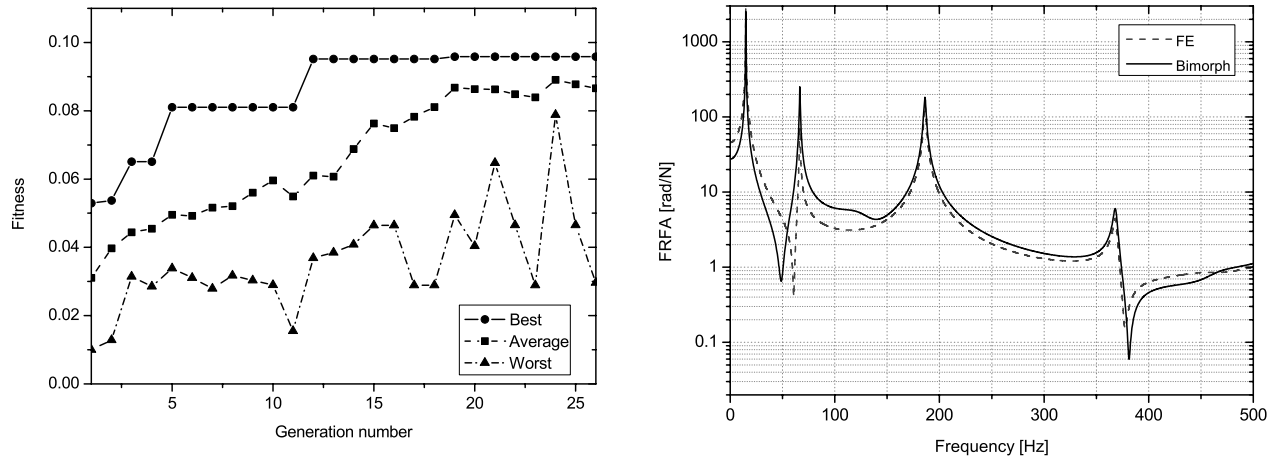

Figure 4. Fitness evolution and comparison between FE (---) and bimorph (—) angular FRFs for beam angular response at 250mm

Notice that we make use of analytical modal shapes with a polynomial order p equal 8.

4.2. Experimental results

Figure 5 shows the basic experimental set-up used during the tests. The test used a PCB impact hammer 086C03 ($2.28\,mV/N$ without extender), a Kistler 8836M01 angular accelerometer (18.5 grams) to measure the angular acceleration, an ICP sensor power unit model 480C02 and a VDC power supply.

Exponential windows were used in both the input and output signals and the angular accelerometer sensor were attached to the beam by a single 10-32 socket head cap screw. 4096 spectral lines were used into the Fourier signal analyzer (SignalCalc® ACE).

Figure 6 shows a comparison between angular FRFs obtained by an angular accelerometer and the numerical results of the bimorph sensor for beam angular response at 250mm and 400mm, respectively.

Notice that in the Fig. 6 the angular FRFs are quite similar but the angular FRF from angular accelerometer does not consider the presence of bimorph, as well as, angular FRF from numerical bimorph does not consider the presence

of the angular accelerometer. Also, the noise that can be seen in the angular receptances is due the accelerometer low sensitivity (about $34\mu V / rad / s^2$) which leads to low signal to noise ratio.

Figure 5. Experimental set-up

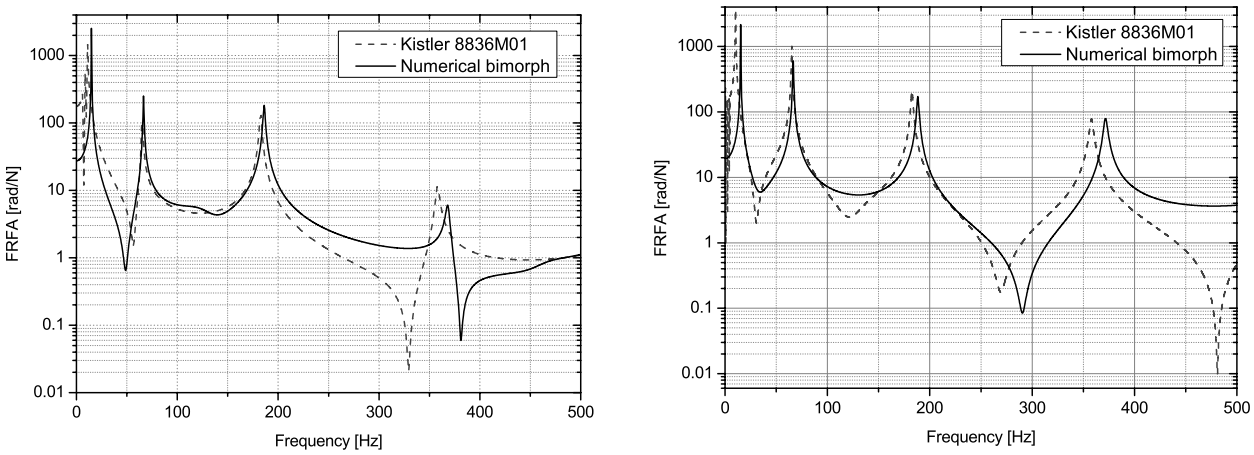

a) $x_{out} = 250$ mm

b) $x_{out} = 400$ mm

Figure 6. Comparison between Kistler 8836M01 (---) and numerical bimorph angular FRFs (—).

5. CONCLUSIONS

In this work, dynamic analysis was proposed to evaluate a piezoceramic bimorph sensor that can provide curvature measurements from which, by interpolation techniques, angular frequency response functions can be determined.

The comparison of the bimorph sensor results to those obtained directly by rotational degrees of freedom included in a finite element model shows that the bimorph sensor is reliable for rotational FRF measurements. The analysis also showed the suitability of the optimization algorithm to obtain optimal locations and size of the bimorph sensor in beam-like structures in order to procure a good agreement between FE results and bimorph results.

Further work will be focused into the optimization of position and length of several bimorph sensors using genetic algorithms for structures like beam and plates.

6. ACKNOWLEDGEMENTS

The authors gratefully acknowledge the support of the FAPESP through a doctoral scholarship award number 04/00264-9.

7. REFERENCES

Algrain, M.C., 1991, “Estimation of 3-D angular motion using gyroscopes and linear accelerometers”. IEEE Transaction on Aerospace and Electronic Systems, Vol. 27, pp. 910-920.

Bello, M., Sestieri, A., DÁmbrogio, W., La Gala, F., 2003, "Development of a Rotation Transducer Based on Bimorph PZTs". Mechanical Systems and Signal Processing, Vol. 17, N. 5, pp. 1069-1081.

Benjeddou, A., Trindade, M.A., Ohayon, R., 1997, "A unified beam finite element model for extension and shear piezoelectric actuation mechanisms". Journal of Intelligent Material Systems and Structures, Vol. 8, N. 12, pp. 1012-1025.

Bokelberg, E. H., Sommer, H.J., Trethewey, M.W., Chu, C-H, 1993, "Simultaneous measurements of six co-ordinate vibration: three translation and three rotations". Proceedings of the 11th International Modal Analysis Conference – IMAC, Kissimee, pp. 522-526.

Cafeo, J.A., Trethewey, M.W., Sommer, H.J., 1992, "Measurement and application of experimental rotational degrees of freedom for mode shape refinement". The International Journal of Analytical and Experimental Modal Analysis, Vol. 7, N. 4, pp. 255-269.

Duarte, M. L. M., Ewins, D.J., 2000, "Rotational degrees of freedom for structural coupling analysis via finite-difference technique with residual compensation". Mechanical Systems and Signal Processing, Vol. 14, N. 2, pp. 205-227.

Laughling, D.R., Andaman, A.A., Sebesta, H.R., 1992, "Intertial Angular Rate Sensors: Theory and Applications". Sensors, pp. 20-24.

Liu, W., Ewins, D.J., 1999, "The Importance Assessment of RDOF in FRF Coupling Analysis". Proceedings of the 17th International Modal Anlysis Conference – IMAC, Kissimmee, pp. 1481-1487.

Ng'andu, A.N., Fox, C. H. J., Williams E.J., 1993, "Estimation of rotational degrees of freedom using curve and surface fitting". Proceedings of the 11th International Modal Analysis Conference – IMAC, Kissimmee, pp. 620-626.

Rahmoune, M., Benjeddou, A., Ohayon, R., Osmont, D., 1998, "New thin piezoelectric plate models". Journal of Intelligent Material Systems and Structures, Vol. 9, N. 12, pp. 1017-1029.

Trindade, M.A., Benjeddou, A., Ohayon, R., 2001, "Finite element modelling of hybrid active-passive vibration damping of multilayer piezoelectric sandwich beams – part I: Formulation". International Journal for Numerical Methods in Engineering, Vol. 51, pp. 835-854.

Varoto, P.S., 1996, "The Rules for the Exchange and Analysis of Dynamic Information in Structural Vibration". Doctoral dissertation, Iowa State University, pp. 233.

Yoshimura, T., Hosoya, N., 2000, "FRF estimation on rotational degree of freedom by rigid block attachment". Proceedings of the International Seminar on Modal Analysis – ISMA 25, Leuven.

8. RESPONSIBILITY NOTICE

The authors are the only responsible for the printed material included in this paper.